

Photothermal diffuse reflectance: a new tool for spectroscopic investigation of scattering samples

J. M. Rey · J. Kottman · M. W. Sigrist

Received: 8 January 2013 / Accepted: 1 April 2013 / Published online: 10 April 2013
© Springer-Verlag Berlin Heidelberg 2013

Abstract A new method named photothermal diffuse reflectance (PTDR) is presented. This method combines the diffuse reflectance spectroscopy with the photothermal technique and is particularly suited for the investigation of strongly scattering samples. This method takes advantage of the high spectral selectivity and absorption of the mid-infrared region with the larger scattering cross section and high detector sensitivity available in the near-infrared. A model describing the PTDR method is proposed and supported with experimental results. The potential of the PTDR technique is illustrated by experimental signals obtained from various scattering media like polymers, liquids and powders.

1 Introduction

Photothermal measurements represent a useful method for characterizing thermal properties such as thermal conductivity and thermal diffusivity of materials [1–3]. Among the photothermal techniques, photothermal reflectance (also called modulated optical reflectance) is an effective non-destructive evaluation technique [4–6]. This method is based on the excitation of the material under investigation with an intensity-modulated laser beam (pump laser) which results in a periodic variation of the local temperature of the sample surface due to the heat produced by the absorbed pump intensity. The temperature change induces a periodic variation of the sample's refractive index at the

modulation frequency of the pump beam intensity. The induced periodic variation of the sample's reflectivity is detected by measuring the modulation of its reflectance using a probe beam (probe laser) that is reflected from the sample surface. Photothermal reflectance methods have proven to be especially valuable for investigating highly opaque materials and have been used extensively in several areas of science and technology, particularly for studies of thermal conductivity of thin films [7], thermal conductance of interfaces [8] and thermal diffusivity of solids [9].

When light reaches a scattering medium, it can be reflected by the surface (specular reflection) or it can enter the medium. The light that enters the medium can then be absorbed, transmitted or scattered. A part of the scattered light can return to the surface and escape the scattering medium leading to diffuse reflectance (also called remittance). A widely used diffuse reflectance scheme employs a laser beam focused to provide a small spot on the surface of the scattering sample and an optical fiber to collect the light remitted at a given distance (typically 2–20 mm) from the laser input spot. One advantage of this scheme is that the whole measurement is conducted from the same side of the sample and thus no access to the rear surface is needed. Diffuse reflectance is an excellent non-destructive sampling tool for powdered and solid materials. It is also widely utilized for medical diagnostic purposes, such as noninvasive optical spectroscopy of various tissues [10–12].

Here we report on the combination the advantages of the photothermal techniques with those of the diffuse reflectance method. This is achieved by exciting the sample with pulsed mid-infrared light which, when absorbed by the sample, generates a temperature increase. The sample is simultaneously irradiated with a second light beam (visible or near-infrared), which is marginally absorbed but strongly scattered by the sample and thus leads to a strong

J. M. Rey · J. Kottman · M. W. Sigrist (✉)
Laser Spectroscopy and Sensing Laboratory,
Institute for Quantum Electronics, ETH Zurich,
Schafmattstrasse 16, 8093 Zurich, Switzerland
e-mail: sigristm@phys.ethz.ch

diffuse reflectance signal. This diffuse reflectance signal is influenced by the absorbed mid-infrared light and thus yields information on the optical and thermal properties of the samples. We call this technique photothermal diffuse reflectance (PTDR). Using two excitation beams has many advantages as it combines the high spectral selectivity and absorption cross section of the mid-infrared region with the stronger scattering cross section and higher detector sensitivity available in the near-infrared. In this work, the PTDR method will be investigated and its potential illustrated by PTDR analyses of various powders, polymers and liquids.

2 Experimental arrangement

Our photothermal diffuse reflectance setup is depicted in Fig. 1. It consists of an external cavity quantum cascade laser (EC-QCL, Daylight Solutions, DLS-TLS-001-PL) generating the pump beam and providing more than 20 mW between 9.17 and 9.88 μm . The EC-QCL beam is interrupted with a shutter to generate 0.5 s long pulses that heat the sample. A temperature-stabilized near-infrared diode laser (785 nm, ADL-78901TX, ca. 20 mW) generates the probe beam and illuminates the scattering sample. This beam is amplitude-modulated at 57.7 kHz frequency to allow a lock-in detection of the scattered light which is collected by a plastic optical fiber (step-index PMMA; diam. = 1 mm) located 0.5 mm above the sample surface. The collected light is fed to a silicon/PIN photodiode (New Focus, Model 1801). The photodiode signal is detected by a lock-in amplifier (Stanford Research, SR830) with a 10 ms time constant and read-out rate of 256 Hz. The mid-infrared laser (pump, beam diameter ca. 3 mm) and the near-infrared laser (probe, beam diameter <0.3 mm) hit the sample at the same location and the centre of both beams is superimposed. The scattered light is collected by the optical fiber located 5 mm apart. The light detection

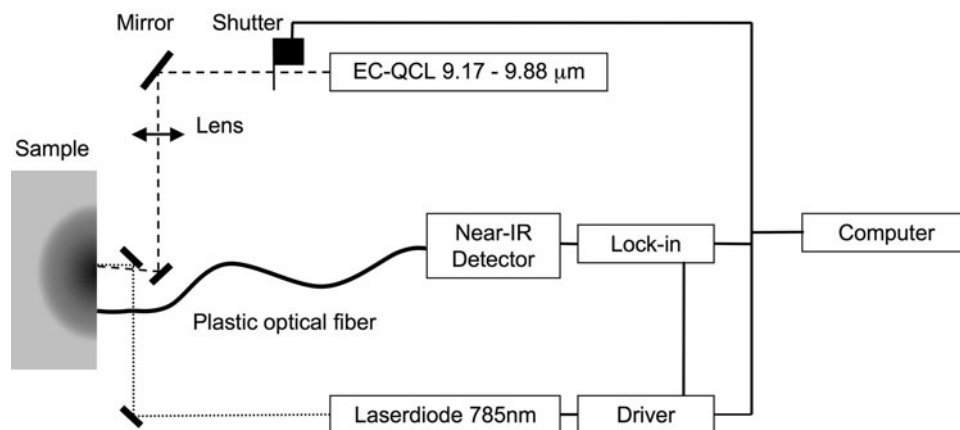
scheme is not sensitive to the mid-infrared light from the pump beam since the plastic optical fiber does not transmit at this wavelength, the silicon detector is not sensitive at this wavelength, and a lock-in detection at 57.7 kHz is used while the mid-infrared beam is pulsed (500 ms, 125 mHz). For each EC-QCL pulse, the signal originating from the lock-in is recorded in the computer and can be averaged, if needed, to improve the signal to noise ratio. The output is a time-dependent signal showing the evolution of the collected diffusely scattered near-infrared light after the EC-QCL pulse (mid-infrared excitation).

3 Results and discussion

A typical PTDR signal obtained with a turbid polyoxymethylene (POM, also called polyacetal) polymer is presented in Fig. 2. The POM sample is irradiated during 500 ms with a 4 mJ pulse at a wavelength of 9.766 μm and the PTDR reflectance signal is recorded during ca. 8 s and subsequently averaged 10 times. The lower dotted line shows the time-dependent signal of the collected scattered near-infrared light without mid-infrared excitation resulting in a flat baseline. The upper line clearly shows an increase of the diffusely scattered light during the mid-infrared pump pulse. The maximum signal is obtained at the end of the pump pulse and amounts to approx. 0.4 % of the base signal (i.e. signal obtained without mid-infrared pump pulse).

The temperature rise at the centre of the spot irradiated by the EC-QCL is approximately 4 K. This estimation is based on the volumetric heat capacity of POM (2.1×10^6 [J m⁻³ K⁻¹] [13]) and neglecting thermal diffusion since the thermal conductivity of POM is low (i.e. 0.25 [W m⁻¹ K⁻¹] [13]) and the heating period relatively short. This 4 K temperature rise corresponds to the observed 0.4 % increase of the diffuse reflectance signal; the experimental sensitivity (i.e. $\Delta(\text{PTDR signal})/\Delta T$) of the

Fig. 1 Schematic representation of the photothermal diffuse reflectance setup



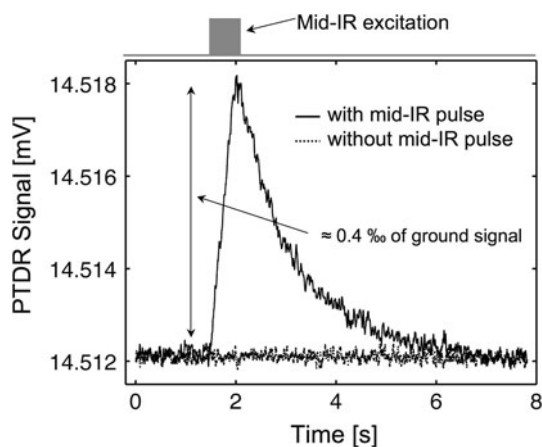


Fig. 2 PTDR signal obtained with a polyoxymethylene (POM) sample (pump wavelength 9.766 μm , pulse duration 500 ms, pulse energy 4 mJ) after 10 averages. The lower line shows the PTDR signal without mid-infrared pulse excitation

PTDR setup is thus $10^{-4} [\text{K}^{-1}]$. The maximum signal amplitude is 6 μV (Fig. 2), while the standard deviation of the background signal is 90 nV. Knowing the temperature rise (i.e. 4 K), the minimum detectable temperature change is estimated to be 0.06 K (1σ , $10\times$ averaging).

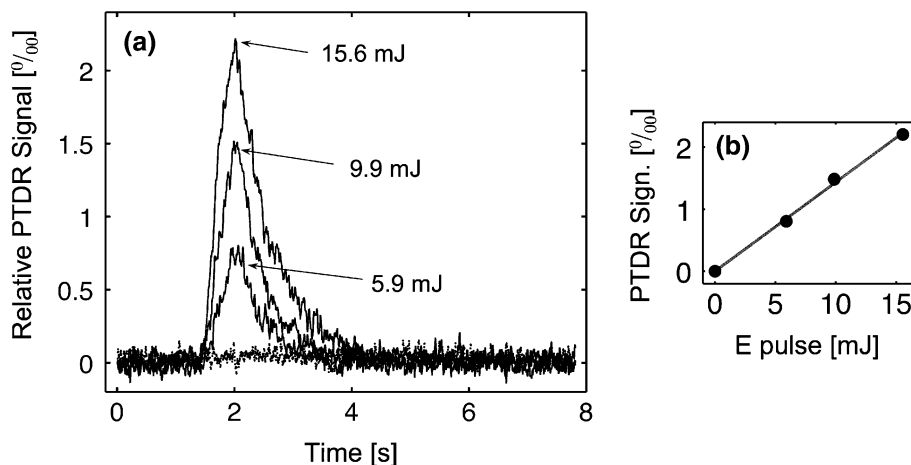
Since the refractive index of the POM sample varies with temperature, its surface reflectivity also changes with temperature. A reduction of the surface reflectivity at the probe beam input point leads to an increased light intensity available for the scattering processes inside the sample and thus to a higher diffuse reflectance signal. A simple model for the PTDR technique can thus be derived: the PTDR signal results from the reflectivity change at the probe beam input spot due to the variation of the reflective index with temperature. Following this model and using typical parameters for a typical polymer (i.e. refractive index = 1.4, $\Delta(\text{refractive index})/\Delta T = -3 \times 10^{-4} [\text{K}^{-1}]$), the sensitivity of the of the PTDR amounts to $0.4 \cdot 10^{-4} [\text{K}^{-1}]$ [2]. A reasonable agreement

between the experimental and the modeled sensitivity is thus obtained.

By dividing the variation of the signals (S) obtained during the PTDR experiment by the background signal (i.e. the signal recorded without pump beam, S_0), the relative PTDR signal (i.e. $(S - S_0)/S_0$) is obtained. This relative PTDR signal is independent on the probe beam power. The relative PTDR signal for various pump pulse energies using a glucose powder as scattering sample is presented in Fig. 3 (pulse duration 500 ms, pump wavelength 9.766 μm). Taking the maximum amplitude of the time-dependent signal as a measure of the PTDR signal, a linear behavior of the PTDR signal with the pump energy is observed (Fig. 3b). This result implies that PTDR signals can be normalized by the energy of the pump pulse. This is of great interest for signal calibration, e.g. if PTDR signals obtained using different pump energies have to be compared (such as PTDR signals recorded for various pump wavelengths and thus pump energies).

Normalized PTDR signals from various samples are presented in Fig. 4. Apart from POM, polytetrafluoroethylene (PTFE) polymer, homogenized milk (3.8 % fat), glucose powder (typical grain diameter 50 μm) and an opal glass diffuser have been measured. All signals have been recorded using a pulse duration of 500 ms and a pump wavelength of 9.766 μm but, depending on the sample, various pulse energies (2.5–25 mJ) have been utilized. All samples show a signal rise during the pump pulse. Weaker signals are obtained with glass and milk. Figure 4 indicates that diverse types of samples like polymers, powders and liquids can be investigated using the PTDR technique as long as they scatter light. Based on the PTDR model presented above, the signal is proportional to the change of the refractive index of the sample. The change of the refractive index is, in turn, proportional to the volumetric expansion coefficient (β , Table 1) multiplied by the temperature variation [2, 3]. A detailed description of the relationships

Fig. 3 a Relative PTDR signals (pulse duration 500 ms, pump wavelength 9.766 μm) obtained with a glucose powder for various pump pulse energies. **b** Dependence of the PTDR signal on the pulse energy, the line shows a linear fit



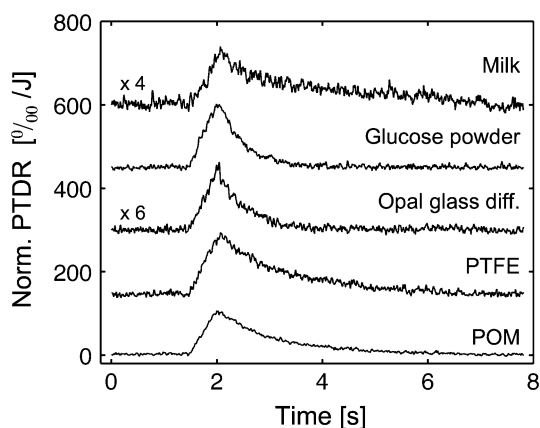


Fig. 4 Normalized PTDR signals from various samples: polyoxymethylene (POM), polytetrafluoroethylene (PTFE), homogenized milk sample (3.8 % fat), glucose powder (typical grain diameter 50 μm) and opal glass diffuser. In all cases, a 500 ms pulse duration and a pump wavelength of 9.766 μm, but various pulse energies have been employed. The opal glass and milk signals have been multiplied by 6 and 4 before plotting, respectively. The signals are vertically shifted for better clarity

Table 1 Literature data of selected thermal properties of the investigated samples

Material	Volumetric heat capacity	Volumetric expansion coefficient	β/C_v	References
	C_v [J m ⁻³ K ⁻¹]	β [K ⁻¹]		
Glass (BK7)	2.2×10^6	25×10^{-6}	11	[18]
Milk	4.0×10^6	200×10^{-6}	50	[19]
PTFE	2.3×10^6	300×10^{-6}	130	[13]
POM	2.1×10^6	300×10^{-6}	143	[13]

These data are utilized to derive the β/C_v ratio that is given in Fig. 5 (see text)

between temperature, refractive index and light transmission can be found in Ref. [3].

This temperature variation (neglecting heat diffusion and assuming a similar irradiated volume) is inversely proportional to the volumetric heat capacity (C_v , Table 1). This results in normalized PTDR signals being proportional to β/C_v . In Fig. 5, the experimental normalized PTDR signals from Fig. 4 are plotted versus β/C_v (Table 1) for the various materials. The reasonable linear behavior observed in Fig. 5 is a further corroboration for the PTDR model given above.

Depending on the pump wavelength, the absorption coefficient (α) of the sample varies. Figure 6 depicts the PTDR signals obtained with a glucose powder at two different pump wavelengths (i.e. 9.766 and 9.434 μm). These two wavelengths are chosen since they correspond to a

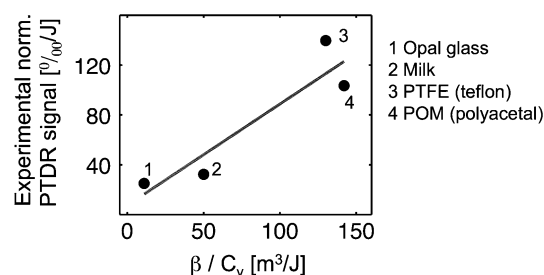


Fig. 5 Experimental normalized PTDR signal (corresponding to Fig. 4) versus β/C_v for the various materials (see text). The line shows a linear fit

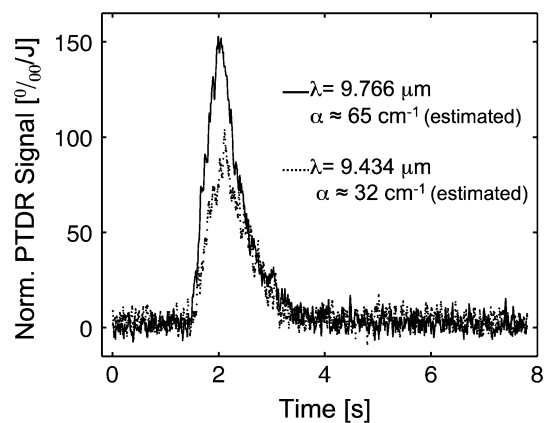


Fig. 6 Normalized PTDR signals at 9.766 and 9.434 μm excitation wavelengths for a glucose powder

significantly different mid-infrared absorption coefficient (estimated to be 65 and 32 cm⁻¹, respectively). These absorption coefficients of the glucose powder are estimated from attenuated total reflection (ATR) measurements using a Fourier-transform infrared (FTIR) spectrometer. The PTDR signal of PTFE at two wavelengths (i.e. 9.174 and 9.852 μm) is shown in Fig. 7. The corresponding absorption coefficients (180 and 100 cm⁻¹, respectively) are

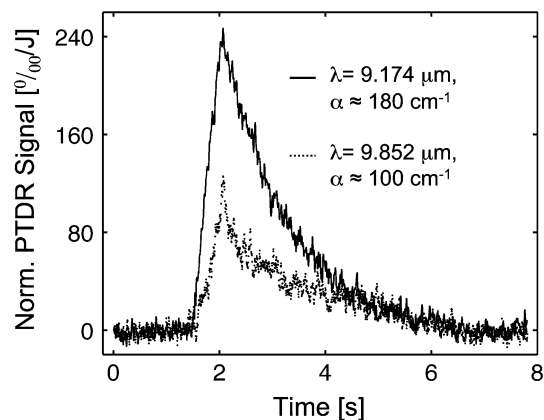


Fig. 7 Normalized PTDR signals at 9.174 and 9.852 μm excitation wavelengths for a PTFE polymer

derived from FTIR measurements conducted in direct transmission with a thin PTFE foil. Figures 6 and 7 demonstrate that the PTDR signal scales with the absorption coefficient and that spectroscopic investigations of scattering materials are feasible using this technique. If the absorption coefficient gets larger, the heat deposited by the pump beam is confined within a smaller volume and the maximum surface temperature gets higher. For a small variation of the absorption coefficients, the PTDR signal is proportional to the absorption coefficient.

4 Conclusion

Using the PTDR method, temperature changes due to light absorption are detected through the variation of the diffuse reflectance. The use of two (i.e. a pump and a probe) wavelengths offers a large choice of applications since each wavelength has its own absorption and scattering cross sections. In this work, this allowed exploiting the benefits of both the mid-infrared high absorption cross section and the strong scattering cross section of the near-infrared. Compared to regular photothermal reflectance spectroscopy, the PTDR technique does not require a flat reflecting surface but can also be successfully implemented on powders. The PTDR technique should also enable to detect temperature changes at the sample surface under vacuum which is not possible using photothermal “mirage effect” [14, 15] or photoacoustic [16, 17] setups. With the PTDR method, the temperature measurement is performed at the location of the probe beam spot, the temperature is thus measured with a high spatial resolution and a mapping of the surface temperature could be done by scanning the surface with the probe beam. The PTDR is a non-contact and non-destructive method for the studies of scattering or turbid samples, which does not require access to the rear sample surface. This method is thus also promising for the study of biological samples like skin.

Acknowledgments The financial support by Glucometrix NIB and ETH Zürich is greatly acknowledged.

References

1. D.P. Almond, P.M. Patel, *Photothermal Science and Techniques* (Chapman & Hall, London, 1996)
2. A. Mandelis, *Photoacoustic and Thermal Wave Phenomena in Semiconductors* (North-Holland, Amsterdam, 1987)
3. S.E. Bialkowski, *Photothermal Spectroscopy Methods for Chemical Analysis* (Wiley, New York, 1996)
4. J. Opsal, M.W. Taylor, W.L. Smith, A. Rosencwaig, *J. Appl. Phys.* **61**, 240 (1986)
5. C. Christofides, I.A. Vitkin, A. Mandelis, *J. Appl. Phys.* **67**, 2815 (1990)
6. G. Langer, J. Hartmann, M. Reichling, *Rev. Sci. Instrum.* **68**, 1510 (1997)
7. R.M. Costescu, M.A. Wall, D.G. Cahill, *Phys. Rev. B* **67**, 054302 (2003)
8. S. Huxtable, D.G. Cahill, V. Fauconnier, J.O. White, J.C. Zhao, *Nat. Mater.* **3**, 298 (2004)
9. K. Hatori, N. Taketoshi, T. Baba, H. Ohta, *Rev. Sci. Instrum.* **76**, 114901 (2005)
10. K. Maruo, M. Tsurugi, M. Tamura, Y. Ozaki, *Appl. Spectr.* **57**, 1236 (2003)
11. A. Cerussi, N. Shah, D. Hsiang, A. Durkin, J.J. Butler, B.J. Tromberg, *J. Biomed. Opt.* **11**, 044005 (2006)
12. P.R. Bargo, S.A. Prahl, T.T. Goodell, R.A. Sleven, G. Koval, G. Blair, S.L. Jacques, *J. Biomed. Opt.* **10**, 034018 (2005)
13. J.A. Dean, *Lange's Handbook of Chemistry* (McGraw-Hill, London, 1999)
14. M.J.D. Low, C. Morterra, A.G. Severdia, M. Lacroix, *Appl. Surf. Sci.* **13**, 429 (1982)
15. A.C. Boccara, D. Fournier, J. Badoz, *Appl. Phys. Lett.* **36**, 130 (1980)
16. A. Rosencwaig, *Photoacoustics and Photoacoustic Spectroscopy* (Wiley, New York, 1980)
17. A.C. Tam, *Ultrasensitive Laser Spectroscopy* (Academic Press, New York, 1983)
18. M.J. Weber (ed.), *Handbook of Optical Materials* (CRC Press, Boca Raton, 2003)
19. P. Walstra, J.T.M. Wouters, T.J. Geurts, *Dairy Science and Technology* (CRC Press, Boca Raton, 2005)